The following publication K. H. Lo, Y. Yang and K. -W. E. Cheng, "Front-End Voltage Regulations of Inductive Power Transfer Systems with Switched LCL Compensators," 2020 8th International Conference on Power Electronics Systems and Applications (PESA), 2020, pp. 1-6 is available at https://doi.org/10.1109/PESA50370.2020.9344018

Front-End Voltage Regulations of Inductive Power Transfer Systems with Switched LCL Compensators

Kwing Hei Lo, Yun Yang, Ka-wai Eric Cheng
Department of Electrical Engineering, The Hong Kong Polytechnic University, Hong Kong
{kwinghei.lo, yun1989.yang, eric-cheng.cheng}@connect.polyu.hk

Abstract–The output voltages are regulated by either the user-end DC regulators or the front-end inverters via wireless communications in conventional non-radiative inductive power transfer (IPT) systems. However, the bulky sizes of the DC regulators and the communication devices may deteriorate the power densities of the receivers. To this end, a communication-free voltage regulation scheme is proposed for an LCL-S compensated IPT system by controlling the switched LCL compensator at the primary side. The output voltage of the IPT system can be estimated by measuring the front-end AC current of the transmitter resonator at the nominal condition without any communication feedbacks. Based on the estimated output voltage, the primary-side controller can automatically switch on the desired compensated inductors, such that the output voltage can track the reference. The proposed scheme is validated by the simulation results in PSIM9.0.

Keywords–Inductive power transfer (IPT), LCL-S compensation, communication-free

I. INTRODUCTION

The electric vehicle (EV) industry has provided a wide range of possibilities for the future transportation [1]–[8]. This occurrence has led researchers to investigate this technology, such as the Inductive Power Transfer (IPT) systems [3]–[8]. Nonetheless, the EV sector is not the only one focused on this particular technology of the IPT technology [9]–[11]: wearables, medicines, applications where the possibility to introduce the human hand is not available, etc. It is due primarily to overly advantage of the total isolation between the primary/transmitter from the secondary/receiver. This fact makes this technology an excellent option for the future of the battery charger systems when the isolation between the power supply and demand is inevitable.

The output voltage regulations of practical IPT systems are implemented by user-end DC regulators or the front-end inverters with the output feedback signals via wireless communications [12]–[18]. A schematic diagram of using a user-end DC regulator to control the output voltage is shown in Fig. 1(a). Obviously, the existence of the DC regulator will increase the receiver size and may require additional power supply for the DC regulator. A schematic diagram of using a wireless communication device to feedback output voltage to the front-end inverter is shown in Fig. 1(b). The wireless communication devices will not only enhance the volume of both the transmitter and the receiver, but also brings additional high cost. Therefore, it is necessary to develop a cost-effective scheme to regulate output voltages of IPT systems without using DC regulators and wireless communication devices.

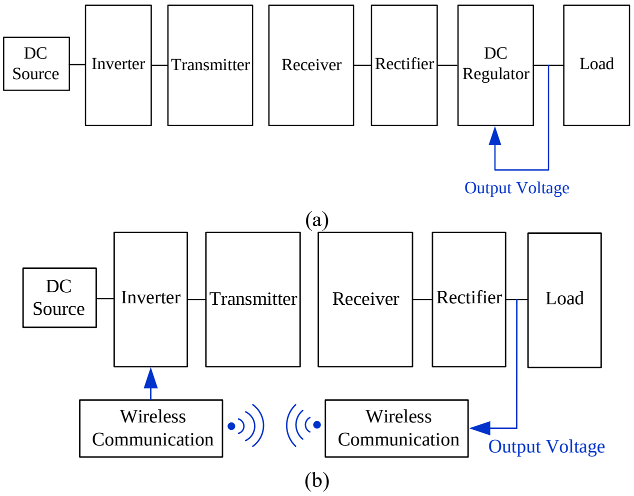

Fig. 1: Timing diagrams of the gate signals for the inverter.

This paper bridges the research gap by introducing a communication-free switched LCL-compensation scheme at the front-end to regulate the output voltage. The LCL-S compensation gains the merits of (i) null reflected reactance, (ii) relatively high efficiency even if the quality factors of the coils are low, (iii) more flexible current operations in either continuous or discontinuous mode, (iv) implementation of unity power factor by variable frequency control, and (v) elimination of reactive loading in high power applications, as compared to the four fundamental compensation schemes (i.e., SS, SP, PS and PP)[19]. Inherited from the conventional LCL-S compensation scheme, the proposed switched LCL-S compensation scheme possesses these aforementioned advantages, whereas extends the controllability by changing the fixed compensated inductor at the primary side to switched compensated inductors in multiple strings. The combinations of these inductor strings render the equivalent impedance of the IPT system alters, such that the output voltage can be regulated.

II. A BRIEF REVIEW OF THE CONVENTIONAL LCL-S COMPENSATED IPT SYSTEMS

The circuit diagram of a conventional LCL-S compensated IPT system is shown in Fig. 2. Here, both the compensated capacitors (i.e., C_p and C_s) are in resonances with the coil inductances (i.e., L_p and L_s), respectively, as

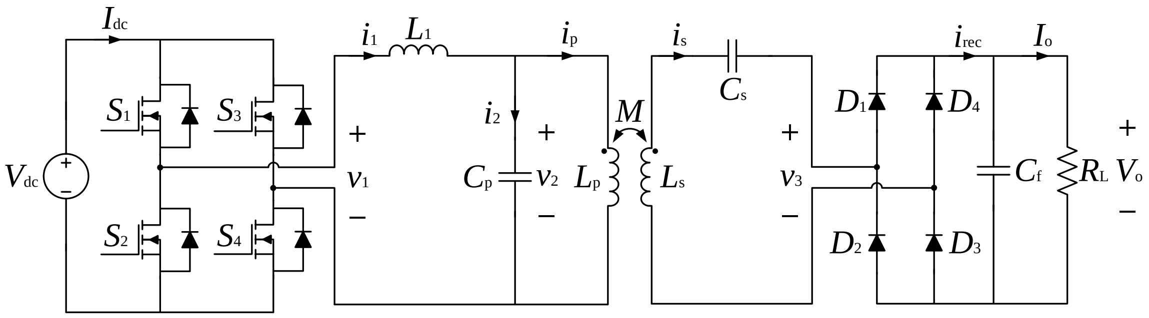

Fig. 2. Circuit diagram of a typical LCL-S compensated IPT system.

$$\omega^2 = \frac{1}{L_\mathrm{p} C_\mathrm{p}} = \frac{1}{L_\mathrm{s} C_\mathrm{s}} \tag{1}$$

where ω is the switching angular frequency. The compensated inductance L_1 equals to the self-inductance of the primary coil (i.e., $L_1 = L_\mathrm{p}$). The switching signals S_1 and S_2, S_3 and S_4 are controlled in complementation and the switching signals S_1 and S_4, S_2 and S_3 are in phase. The timing diagrams of the four gate signals are depicted in Fig. 3.

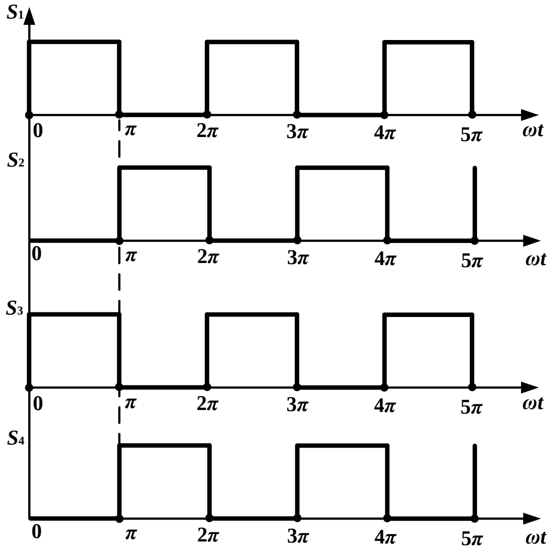

Fig. 3: Timing diagrams of the gate signals for the inverter.

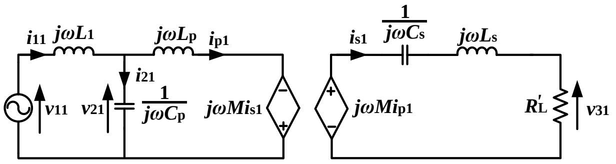

Fig. 4. Equivalent circuit of the conventional LCL-S compensated IPT system.

Based on the circuit diagram in Fig. 2, an equivalent circuit of the conventional LCL-S compensated IPT system can be depicted, as shown in Fig. 4. Here, the parameters v_{11}, i_{11}, i_{21}, v_{21}, $i_{\mathrm{p}1}$, $i_{\mathrm{s}1}$, and v_{31} are the fundamental components of v_1, i_1, i_2, v_2, i_p, i_s, and v_3, respectively. According to the Fourier analysis, the peak values of the v_{11}, i_{11}, v_{31}, and $i_{\mathrm{s}1}$, i.e., V_{11}, I_{11}, V_{31}, and $I_{\mathrm{s}1}$ satisfy

$$V_{11} = \frac{4}{\pi} V_\mathrm{dc} \tag{2.1}$$

$$I_{11} = \frac{\pi}{2} I_\mathrm{dc} \tag{2.2}$$

$$V_{31} = \frac{4}{\pi} V_\mathrm{o} \tag{2.3}$$

$$I_{\mathrm{s}1} = \frac{\pi}{2} I_\mathrm{o} \tag{2.4}$$

Besides, the equivalent load resistance R_L' satisfies

$$R_L' = \frac{8}{\pi^2} R_\mathrm{L} \tag{2.5}$$

Based on the equivalent circuit and the Kirchhoff's laws,

$$v_{11} = j\omega L_1 i_{11} + \left(i_{11} - i_{\mathrm{p}1}\right) \frac{1}{j\omega C_\mathrm{p}} \tag{3.1}$$

$$j\omega M i_{\mathrm{p}1} = \left(j\omega L_\mathrm{s} + \frac{1}{j\omega C_\mathrm{s}} + R_L'\right) i_{\mathrm{s}1} \tag{3.2}$$

Due to the compensated inductance L_1 is designed to equalize the primary coil (i.e., $L_1 = L_\mathrm{p}$), by substituting (1) into (3.1) and (3.2), respectively,

$$v_{11} = -\frac{i_{\mathrm{p}1}}{j\omega C_\mathrm{p}} \tag{4.1}$$

$$j\omega M i_{\mathrm{p}1} = R_L' i_{\mathrm{s}1} \tag{4.2}$$

By substituting (4.1) into (4.2) to eliminate $i_{\mathrm{p}1}$,

$$i_{\mathrm{s}1} = \frac{M}{L_\mathrm{p} R_L'} v_{11} \tag{5.1}$$

and

$$v_{31} = \frac{M}{L_\mathrm{p}} v_{11} \tag{5.2}$$

Based on (5.1) and (5.2), the amplitudes of the parameters hold

$$I_{\mathrm{s}1} = \frac{M}{L_\mathrm{p} R_L'} V_{11} \tag{6.1}$$

$$V_{31} = \frac{M}{L_\mathrm{p}} V_{11} \tag{6.2}$$

By substituting (2.1), (2.3), (2.4) and (2.5) into (6.1) and (6.2),

$$I_\mathrm{o} = \frac{M}{L_\mathrm{p} R_\mathrm{L}} V_\mathrm{dc} \tag{7.1}$$

$$V_\mathrm{o} = \frac{M}{L_\mathrm{p}} V_\mathrm{dc} \tag{7.2}$$

Apparently, the output voltage of the system depends on the self-inductance of the primary coil (i.e., L_p), mutual inductance (i.e., M), and the input DC voltage (i.e., V_dc). The output current of the conventional LCL-S compensated IPT system also depends on the load resistance (i.e., R_L).

III. IPT SYSTEMS WITH THE PROPOSED SWITCHED LCL-S COMPENSATORS

By changing the fixed compensated inductor L_1 in Fig. 2 to switched compensated inductors (as shown in Fig. 5), the equivalent impedance of the IPT system can be controlled by the switches in series with the compensated inductors (i.e., $S_{\mathrm{L}1}$, $S_{\mathrm{L}2}$,…,$S_{\mathrm{L}n}$). By assuming the switched compensated inductors as an equivalent compensated inductor L_x, an equivalent circuit of the IPT system with the switched LCL-S compensator can be plotted, as shown in Fig. 6.

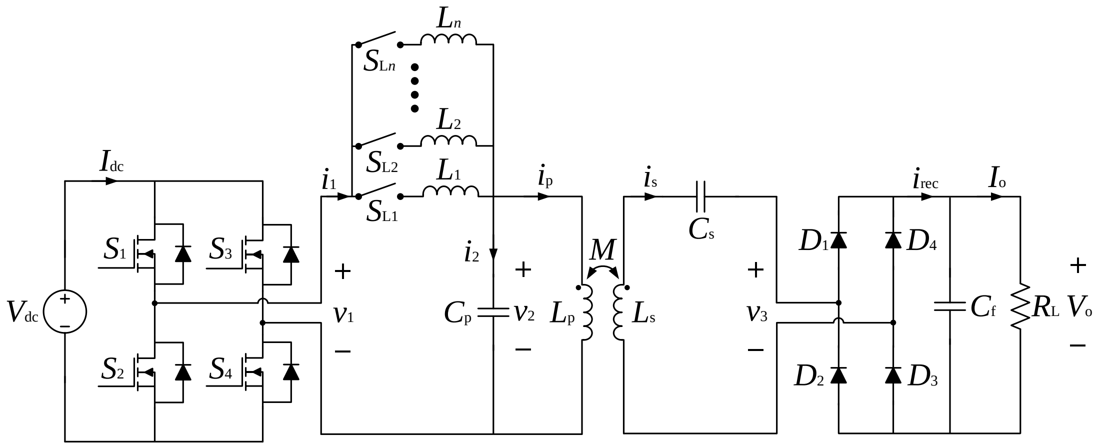

Fig. 5. Circuit diagram of the IPT system with the proposed switched LCL-S compensator.

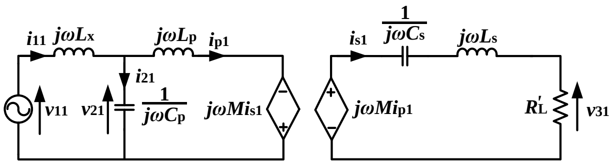

Fig. 6. Equivalent circuit of the IPT system with the switched LCL-S compensator.

Based on the equivalent circuit and the Kirchhoff's laws,

$$v_{11} = j\omega L_x i_{11} + \left(i_{11} - i_{\mathrm{p}1}\right)\frac{1}{j\omega C_{\mathrm{p}}} \tag{8.1}$$

$$\left(i_{11} - i_{\mathrm{p}1}\right)\frac{1}{j\omega C_{\mathrm{p}}} = j\omega L_{\mathrm{p}} i_{\mathrm{p}1} - j\omega M i_{\mathrm{s}1} \tag{8.2}$$

$$j\omega M i_{\mathrm{p}1} = \left(j\omega L_{\mathrm{s}} + \frac{1}{j\omega C_{\mathrm{s}}} + R_L'\right) i_{\mathrm{s}1} \tag{8.3}$$

By substituting (8.2) and (8.3) into (8.1) to eliminate i_{11} and $i_{\mathrm{p}1}$,

$$i_{\mathrm{s}1} = \frac{1}{\frac{8L_{\mathrm{p}}R_{\mathrm{L}}}{\pi^2 M} + \omega M\left(\frac{L_{\mathrm{x}}}{L_{\mathrm{p}}} - 1\right)j} v_{11} \tag{9.1}$$

$$v_{31} = \frac{1}{\frac{L_{\mathrm{p}}}{M} + \frac{\pi^2 \omega M}{8R_{\mathrm{L}}}\left(\frac{L_{\mathrm{x}}}{L_{\mathrm{p}}} - 1\right)j} v_{11} \tag{9.2}$$

Based on (5.1) and (5.2), the amplitudes of the parameters hold

$$I_{\mathrm{s}1} = \frac{1}{\sqrt{\left(\frac{8L_{\mathrm{p}}R_{\mathrm{L}}}{\pi^2 M}\right)^2 + \omega^2 M^2\left(\frac{L_{\mathrm{x}}}{L_{\mathrm{p}}} - 1\right)^2}} V_{11} \tag{10.1}$$

$$V_{31} = \frac{1}{\sqrt{\left(\frac{L_{\mathrm{p}}}{M}\right)^2 + \left(\frac{\pi^2 \omega M}{8R_{\mathrm{L}}}\right)^2\left(\frac{L_{\mathrm{x}}}{L_{\mathrm{p}}} - 1\right)^2}} V_{11} \tag{10.2}$$

By substituting (2.1), (2.3), (2.4) and (2.5) into (10.1) and (10.2),

$$I_{\mathrm{o}} = \frac{\frac{8}{\pi^2}}{\sqrt{\left(\frac{8L_{\mathrm{p}}R_{\mathrm{L}}}{\pi^2 M}\right)^2 + \omega^2 M^2\left(\frac{L_{\mathrm{x}}}{L_{\mathrm{p}}} - 1\right)^2}} V_{\mathrm{dc}} \tag{11.1}$$

$$V_{\mathrm{o}} = \frac{1}{\sqrt{\left(\frac{L_{\mathrm{p}}}{M}\right)^2 + \left(\frac{\pi^2 \omega M}{8R_{\mathrm{L}}}\right)^2\left(\frac{L_{\mathrm{x}}}{L_{\mathrm{p}}} - 1\right)^2}} V_{\mathrm{dc}} \tag{11.2}$$

By taking partial derivative of V_o over L_x in (11.2),

$$\frac{\partial V_{\mathrm{o}}}{\partial L_{\mathrm{x}}} = \frac{\frac{V_{\mathrm{dc}}}{L_{\mathrm{p}}^2}\left(\frac{\pi^2 \omega M}{8R_{\mathrm{L}}}\right)^2 (L_{\mathrm{p}} - L_{\mathrm{x}})}{\left[\left(\frac{L_{\mathrm{p}}}{M}\right)^2 + \left(\frac{\pi^2 \omega M}{8R_{\mathrm{L}}}\right)^2\left(\frac{L_{\mathrm{x}}}{L_{\mathrm{p}}} - 1\right)^2\right]^{\frac{3}{2}}} \tag{12}$$

Based on the derivations in (11.2) and (12), a plot of V_o versus L_x can be depicted as shown in Fig. 7. The maximum output voltage (i.e., $V_{\mathrm{omax}} = \frac{M}{L_{\mathrm{p}}} V_{\mathrm{dc}}$) can be achieved by controlling the equivalent compensated inductance equaling the inductance of the primary coil (i.e., L_x=L_p). When the output voltage is required to be less than the maximum value, the equivalent compensated inductance is controlled based on (11.2) by switching on proper inductor strings. The mutual inductance and the load resistance can be preliminarily measured or estimated using the identification methods in [17].

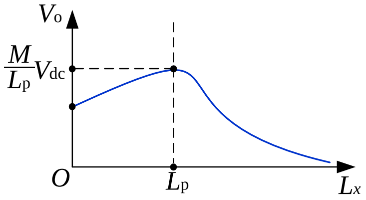

Fig. 7. Plot of V_o versus L_x for the IPT system.

IV. SIMULATION RESULTS

Simulations are conducted in PSIM 9.0. The parameters of the IPT system are listed in Table 1. Initially, the conventional LCL-S compensation is adopted, whereas the compensated inductance (i.e., L_x) is changed with different parameters. The simulated curves of the output voltage (i.e., V_o) versus the compensated inductance (i.e., L_x) for different load and mutual inductance conditions are plotted in Fig. 8. Apparently, the simulated curves are similar to the analytical curve in Fig. 7.

Table 1: Specifications of the IPT system in simulation

Parameters	Symbols	Values
Nominal frequency	f_0	100 kHz
DC voltage source	V_{dc}	21 V
Transmitter coil inductance	L_p	49.2 μH
Receiver coil inductance	L_s	49.2 μH
Transmitter compensated capacitance	C_p	51.484 nF
Receiver compensated capacitance	C_s	51.484 nF
Filter capacitance	C_f	100 μF
Nominal load resistance	R_L	1 Ω
Nominal mutual inductance	M	9.84 μH

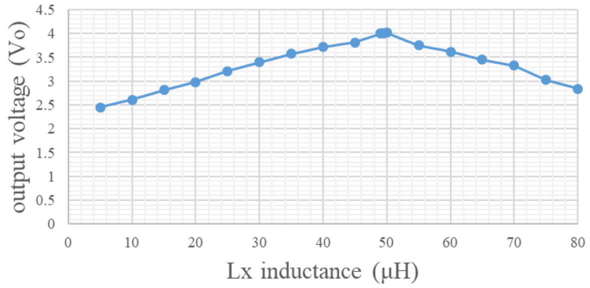

(a) nominal mutual inductance and nominal load resistance

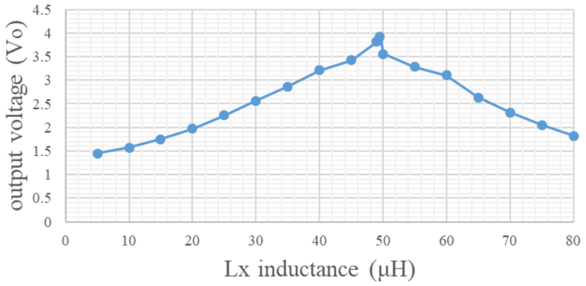

(b) nominal mutual inductance and R_L=0.5 Ω

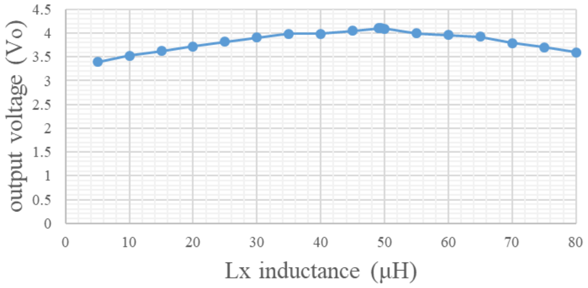

(c) nominal mutual inductance and R_L=2 Ω

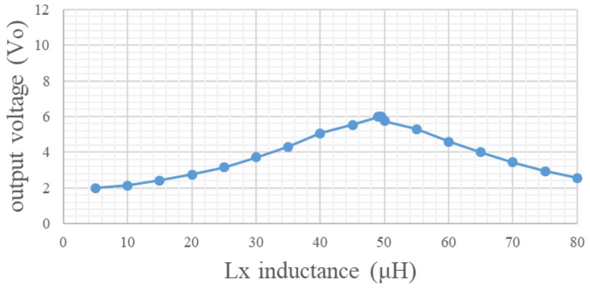

(d) M=14.76 μH and nominal load resistance

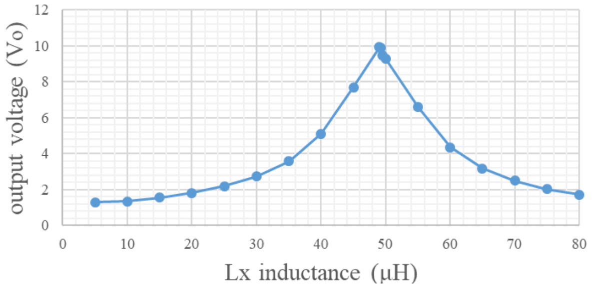

(e) M=24.6 μH and nominal load resistance

Fig. 8. Simulated curves of V_o versus L_x for different load and mutual inductance conditions.

Then, a switched compensator with three compensated inductor strings are adopted. The inductances of the three strings are L_1=38 μH, L_2=46 μH and L_3=1.2 mH, respectively. By controlling the switches S_{L1}, S_{L2} and S_{L3}, the output voltage of the IPT system can be regulated. Three cases with different mutual inductances and load conditions are investigated, as provided in Table 2. In case 1, both the mutual inductance and load condition are nominal. The output voltage reference is changed from 3 V to 3.5 V. In case 2, the mutual inductance is nominal, whereas the load resistance is 0.5 Ω. The output voltage reference is changed from 3 V to 2 V. In case 3, the load condition is nominal while the mutual inductance is 24.6 μH. The output voltage reference is altered from 4 V to 8 V.

Table 2: Case studies of the IPT system with three compensated inductor strings

Case number	Mutual inductance (μH)	Load resistance (Ω)	Output voltage reference (V)
1	9.84	1 Ω	3 V→ 3.5 V
2	9.84	0.5 Ω	3 V→ 2 V
3	24.6	1 Ω	4 V→ 8 V

Fig. 9 show the waveforms of the switching signals S_{L1}, S_{L2} and S_{L3} and the corresponding output voltages of the IPT system in the three cases. In case 1, all the switches S_{L1}, S_{L2} and S_{L3} are ON at the beginning. At the time t=0.01 s, the switch S_{L2} is turned OFF while the switches S_{L1} and S_{L3} are still ON. Accordingly, the output voltage of the system is changed from 3 V to 3.53 V. Obviously, it is well-regulated to track the reference. The corresponding currents of i_1, i_{Lp}, and i_{Ls} are shown in Fig. 9(a). In case 2 (as shown in Fig. 9(b)), the switch S_{L1} is ON while the switches S_{L2} and S_{L3} are OFF initially. At the time t=0.01 s, all the three switches are ON. Accordingly, the output voltage of the system is changed from 2.954 V to 1.995 V. Apparently, the output voltage is also well-regulated to track the reference in case 2. Similarly, in case 3 (as shown in Fig. 9(c)), the output voltage is controlled from 3.97 V to 8.02 V, which tracks the reference accurately.

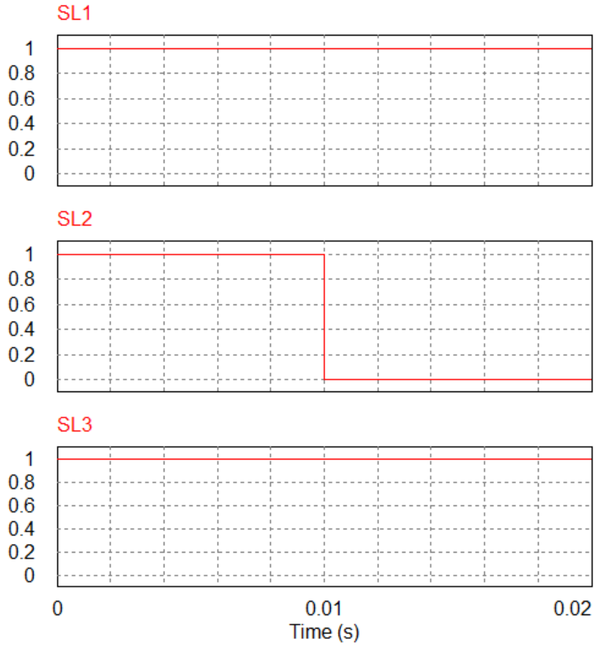

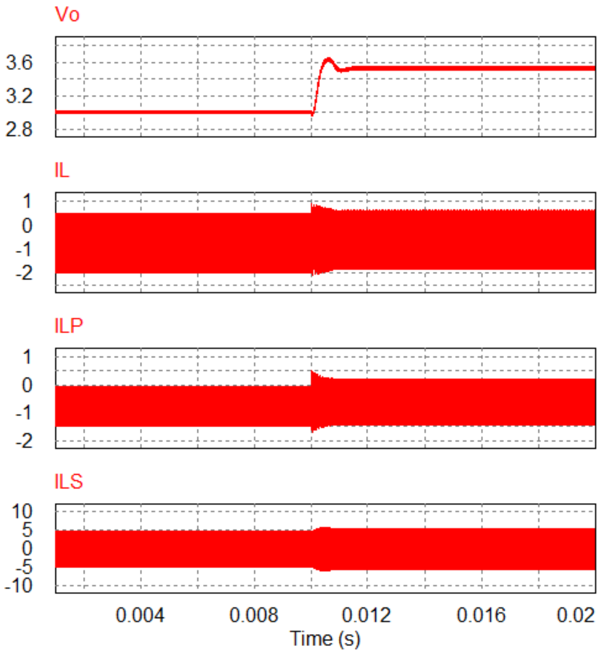

(a) case 1

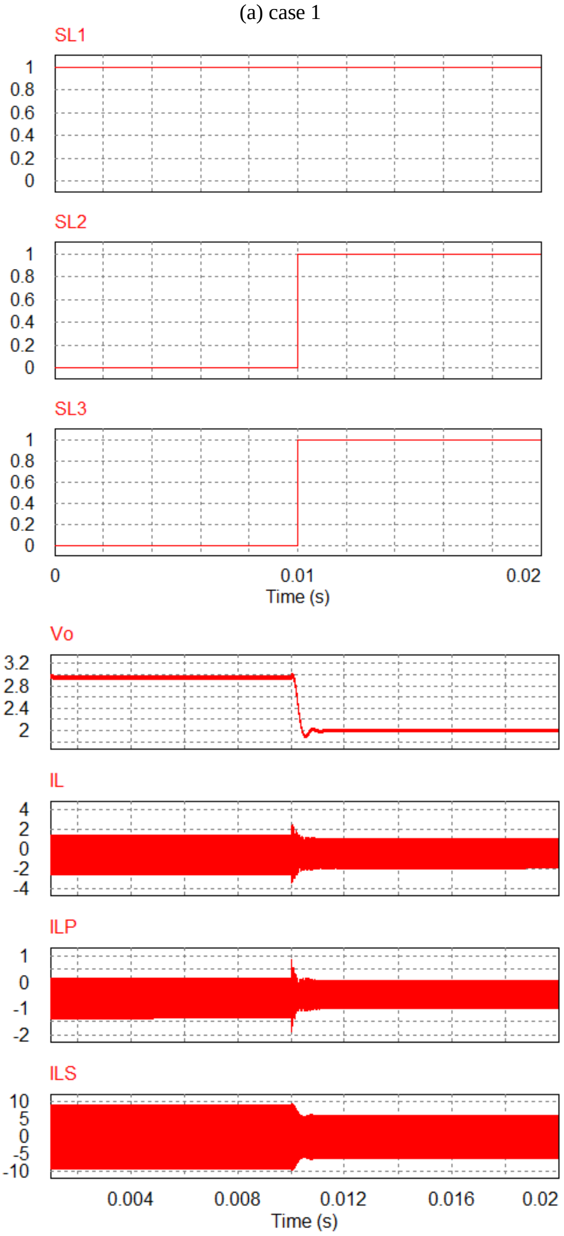

(b) case 2

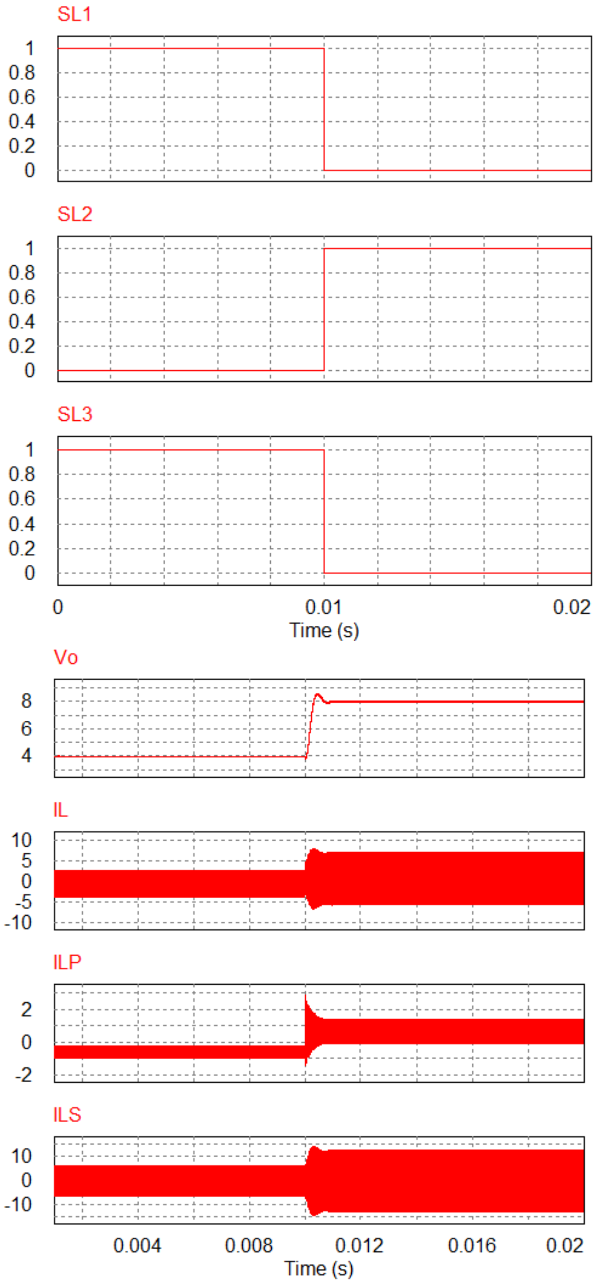

(c) case 3

Fig. 9. Simulated waveforms of the switching signals and the output voltages of the IPT system with the three compensated inductor strings.

V. CONCLUSION

In this paper, switched compensated inductor strings are proposed to substitute the fixed compensated inductor of the classic LCL-S compensation for IPT systems to regulate the output voltages at the front-end without using wireless communications between the transmitters and the receivers. The proposed scheme can improve the power densities of the receivers of the IPT systems by eliminating the bulky DC regulators and communication devices. Simulation results have validated the mathematical relationships between the output voltages and the compensated inductances. The output voltages are also validated to track the references accurately in different mutual inductance and load conditions.

REFERENCES

[1] C. Chan, K. Chau, et al., *Modern electric vehicle technology*, no. 47, Oxford University Press on Demand, 2001.

[2] C. D. Xu and K. W. E. Cheng, “All-electric intelligence anti-lock braking controller for electric vehicle under complex road condition,” in *Int. Symp. Electr. Eng. (ISEE)*, Dec. 2016, 1-5.

[3] G. Covic and J. T. Boys, “Inductive power transfer,” *Proc. of IEEE*, vol. 101, no. 6, pp. 1276-1289, Jun. 2013.

[4] A. W. Green and J. T. Boys, “10 kHz inductively coupled power transfer-concept and control,” in *Proc. 5th Int. Conf. Power Electron. Variable-Speed Drives*, 1994, pp. 694-699.

[5] G. A. J. Elliott, J. T. Boys, and A. W. Green, “Magnetically coupled systems for power transfer to electric vehicles,” in *Proc. Int. Conf. Power Electron. Drives Syst.*, 1995, vol. 2, pp. 797-801.

[6] J. R. Severns, E. Yeow, G. Woody, J. Hall, and J. Hayes, “An ultra-compact transformer for a 100 W to 120 kW inductive coupler for electric vehicle battery charging,” in *Proc. 11th Annu. IEEE Appl. Power Electron. Conf. Expo.*, 1996, vol. 1, pp. 32-38.

[7] J. T. Boys, G. A. Covic, and A. W. Green, “Stability and control of inductively coupled power transfer systems,” *Inst. Electr. Eng. Proc.—Electr. Power Appl.*, vol. 147, no. 1, pp. 37-43, 2000.

[8] J. T. Boys, G. A. J. Elliott, and A. W. Green, “An appropriate magnetic coupling co-efficient for the design and comparison of ICPT pickups,” *IEEE Trans. Power Electron.*, vol. 22, no. 1, pp. 333-335, Jan. 2007.

[9] P. Si, A. P. Hu, S. Malpas, and D. Budgett, “A frequency control method for regulating wireless power to implantable devices,” *IEEE Trans. on Bio. Circuits and Syst.*, vol. 2, pp. 22–29, Mar. 2008.

[10] X. Li, C. Tsui, and W. Ki, “A 13.56 MHz wireless power transfer system with reconfigurable resonant regulating rectifier and wireless power control for implantable medical devices,” *IEEE J. of Solid- State Circuits*, vol. 50, pp. 978–989, Apr. 2015.

[11] U. Jow and M. Ghovanloo, “Design and optimization of printed spiral coils for efficient transcutaneous inductive power transmission,” *IEEE Trans. on Bio. Circuits and Syst.*, vol. 1, pp. 193–202, Sept. 2007.

[12] Y. Yang, W. X. Zhong, S. Kiratipoonvoot, S. C. Tan, and S. Y. R. Hui, “Dynamic improvement of series-series compensated wireless power transfer systems,” *IEEE Trans. Power Electron.*, vol. 33, no. 7, pp. 6351-6360, Jul. 2018.

[13] Y. Yang, S. C. Tan, and S. Y. R. Hui, “Communication-free control scheme for Qi-compliant wireless power transfer system,” in *Energy Conversion Congress and Exposition (ECCE)*, Sept. 2019, pp. 4955-4960.

[14] W. Zhang, S. C. Wong, C. K. Tse and Q. Chen, “Analysis and comparison of secondary series- and parallel-compensated inductive power transfer systems operating for optimal efficiency and load-independent voltage-transfer ratio,” *IEEE Trans. Power Electron.*, vol. 29, no. 6, pp. 2979-2990, Jun. 2014.

[15] Y. Yang, Y. Jiang, S. C. Tan, and S. Y. R. Hui, “A freqeuncy-sweep based load monitoring method for weakly-coupled series-series compensated wireless power transfer systems,” in *IEEE PELS Workshop on Emerging Technologies: Wireless Power Trasnfer (WoW)*, Jun. 2018, pp. 1-5.

[16] K. Aditya and S. S. Williamson, “Design guidelines to avoid bifurcation in a series–series compensated inductive power transfer system,” *IEEE Trans. Ind. Electron.*, vol. 66, no. 5, pp. 3973-3982, May 2019.

[17] Y. Yang, S. C. Tan, and S. Y. R. Hui, “Front-end parameter monitoring method based on two-layer adaptive differential evolution for SS-compensated wireless power transfer systems,” *IEEE Trans. Ind. Informat.*, vol. 15, no. 11, pp. 6101-6113, Nov. 2019.

[18] Y. Yang, S. C. Tan, and S. Y. R. Hui, “Fast hardware approach to determining mutual coupling of series-series-compensated wireless power transfer systems with active rectifiers,” *IEEE Trans. Power Electron.*, vol. 35, no. 10, pp. 11026-11038, Oct. 2020.

[19] C. Jiang, K. T. Chau, C. Liu, and C. H. T. Lee, “An overview of resonant circuits for wireless power transfer,” *Energies*, vol. 10, no. 7, pp. 894, Jun. 2017.